Vertical Ozone Profile over Tibet Using Sage I and II Data①

Zou Han (邹 捍) and *Gao Yongqi* (郜永祺)
Institute of Atmospheric Physics, Chinese Academy of Sciences, Beijing 100029
Received December 17, 1996; revised December 29, 1996

ABSTRACT

This paper discusses the vertical ozone distribution over Tibet using SAGE I and SAGE II data. The annual and seasonal vertical ozone profiles in 10.5–50.5 km a.s.l. over Tibet are analyzed to understand the vertical structure of low ozone value in this region. Regarding to the local ozone deficit, these profiles are compared with the vertical ozone distribution in the non-mountain areas at the same latitudes. The summer low ozone and the May maximum ozone deficit are detected from the SAGE data. The largest ozone deficit in May is found in 15.5–20.5 km a.s.l. centered at 16.5 km over this region. This ozone deficit can be related to the upward mass transfer described by potential temperature variation over Tibet.

Key words: Vertical ozone, Tibet, SAGE, Mass transfer

I. INTRODUCTION

Ozone is one of the greenhouse gases that modify the radiative structure of our atmosphere. A change in ozone amount and distribution can, therefore, influence the climate. In addition, ozone protects the biosphere from the harmful solar ultraviolet radiation. Ozone is continuously being produced and destroyed mainly by solar ultraviolet radiation. Additionally ozone is destroyed by catalytic reactions of nitrogen, hydrogen, chlorine, and bromine oxides. In the early 1970s, it was predicted that the human activities will lead to a diminishing of the ozone layer (Johnston, 1971; Molina et al., 1974). Since the detection of the Antarctica ozone hole by Farman et al. (1985), the downward trend in the column total ozone has been well documented for the regions inside and outside of Antarctica. For example, Bojkov et al. (1990), Reinsel et al. (1994) and Stolarski et al. (1992) showed, from the ground-based and satellite observations, decreases of total ozone in mid-latitudes in both the southern and Northern Hemispheres.

Zhou and Luo (1994) revealed a region of low ozone existing over the Tibetan Plateau in summer. Zou (1996) described the seasonal variations of total ozone and its local deficit over the Tibetan Plateau, using data from the Total Ozone Mapping Spectrometer (TOMS) on board Nimbus 7. Zou's work concluded: 1. Low ozone perturbations exist over the Tibetan Plateau, the Rocky Mountains and the Andes Mountains with largest ozone deficits occurring over Tibet. The low ozone perturbations are stronger in summer than in winter; 2. The monthly ozone concentrations over Tibet have a maximum in March and a minimum in October as 315.4 DU and 273.1 DU, respectively; 3. The local ozone deficit (zonal ozone deviation) in Tibet is strongest (−23.6 DU) in May and weakest (−1.9 DU) in December. The local

①This work is supported by the National Natural Science Foundation of China.

ozone deficit over Tibet is strongly correlated to the surface heat flux to the air in this region with correlation coefficient −0.97; and 4. The annual trend of total ozone in Tibet was −0.79 ± 0.82 DU / year (−2.7 ± 2.8 percent / decade) in 95% confidence during 1979−1991. The seasonal trends of total ozone over Tibet were in range of −0.17 DU / year (−0.6 percent / decade) and −1.79 DU / year (−6.0 percent / decade). As well documented (WMO, 1985), the vertical ozone distribution has maximum concentration in the lower stratosphere, and the ozone variation at different altitudes is governed by different chemical and dynamic mechanisms. For instance, in the dynamic sector, the ozone transport is controlled by atmospheric tide and Kelvin wave above 50 km a.s.l., by planetary waves in c.a. 15−50 km a.s.l., and by synoptic scale motions, planetary waves, cumulonimbus, Walker and Hadley cells etc. below 15 km. Therefore, to help our understanding the mechanism of the ozone deficit in Tibet, it is important to exam how ozone is distributed vertically over Tibet and at which altitude ozone losses. This study is going to give a description of the ozone concentration, seasonal variation and local deficit in Tibet in a manner of vertical distribution. In addition, the potential temperature profiles are analyzed for understanding the impact of vertical mass transfer on the ozone deficit.

II. DATA AND ANALYSIS METHOD

Ozone data used in this study are from the Stratospheric Aerosol and Gas Experiment (SAGE I) instrument on the Applications Explorer Mission−2 (AEM−2) and the Stratospheric Aerosol and Gas Experiment (SAGE II) instrument on Earth Radiation Budget Satellite (ERBS). The 0.600 (m channel, which is near the center of the Chappuis ozone band, is the primary channel used for ozone measurement. The orbital characteristics of SAGE I and SAGE II provide low− and mid−latitude coverage of ozone measurements. Each instrument observes one sunrise and one sunset per orbit. SAGE I measurement has 15 sunrise and 15 sunset events per day. SAGE I events offer latitudinal sweep ranges of approximately 130 degrees within a 4−week period. In addition, they provide global coverage from 72 degrees north to 72 degrees south during a year. Successive observations of the same type are separated by approximately 24 degrees longitude. SAGE II has spatial coverage similar to that of SAGE I, but the coverage is provided from 80 degrees S to 80 degrees N annually. The spatial resolution of the SAGE I and SAGE II data sets is the same. The 1 micrometer wavelength measurement has a vertical resolution of 1 km below 25 km and a resolution of 5 km above 25 km. The vertical resolution of the 0.45 micrometer wavelength channel is 3 km below 25 km. The horizontal resolution is about 250 km for all wavelengths. SAGE I data collection began on February 21, 1979 and continued until November 18, 1981. SAGE II data collection began on October 5, 1984 and continues to the present time. Each satellite instrument makes two ozone profile determinations per orbit (96−97 minutes). Each event is separated by approximately 24 degrees of longitude. SAGE I and SAGE II have 15 orbits per day (NASA, 1992). The validation on SAGE measurements was made by Attmannspacher (1989) and Cunnold (1989). Due to the data supply and quality, the data set used here is from 10.5 to 50.5 km a.s.l. with 1 km resolution, in the period of March 1979 to November, 1981 (SAGE I) and November, 1984 to November, 1989 (SAGE II). The vertical temperature and pressure profiles are supplied by NCAR / NMC.

Because of the satellite orbit characteristics, there are only a few June and August−month observations available over the region concerned. A linear interpolation is applied to obtain data for these months. To derive the spatial−mean vertical profiles in Tibet and a non−mountain zone at the same latitudes, an area weighted mean (cos[latitude] weighted average) is applied in domains, 25−40°N and

75–105°E, and the 25–40°N belt without the regions of the Tibetan Plateau (75–105°E) and the Rocky Mountains (100–115°W), respectively. The local ozone deficit over Tibet is made by subtracting non-mountain zone ozone from the Tibet ozone. $\rho_0 = 2.144 \times 10^{-3} g/cm^3$ is used as the standard ozone density at sea level pressure and temperature in the vertical integration (Wang, 1985) for obtaining the column total ozone in 14.5–50.5 km. The potential temperature is calculated from the equation $\theta = T(1013/p)^{R/C_p}$, where θ is the potential temperature in K, T the air temperature in K, p the air pressure in hPa, R = 287 $Jkg^{-1}K^{-1}$ the gas constant for dry air, and C_p = 1004 $Jkg^{-1}K^{-1}$ the specific heat at constant pressure. In addition, to reveal the realistic figure of ozone distribution, it should be stressed that not any smoothing method is applied in the drawings of this work.

III. RESULTS AND DISCUSSION

1. *Average Vertical Ozone Profile*

In Zou's (1996) study using the Total Ozone Mapping Spectrometer (TOMS) data, it is revealed that there is a low ozone perturbation and local ozone deficit (comparing with the zonal averaged total ozone) over Tibet on a year-round basis. To illustrate the vertical structure of ozone concentration over Tibet, the area weighted mean values in domain of 25–40°N and 75–105°E are calculated from SAGE I and II data for each month and altitude (km). Making a time average, the year-round mean profile over Tibet is obtained. Applying the same procedure for the non-mountain zone (25–40°N zone without Tibet and the Rocky regions), the mean profile in the non-mountain zone is calculated. Subtracting the non-mountain profile from the Tibet one, the local ozone deficit profile is gained. The three profiles associated with the measurement errors are plotted in Fig. 1.

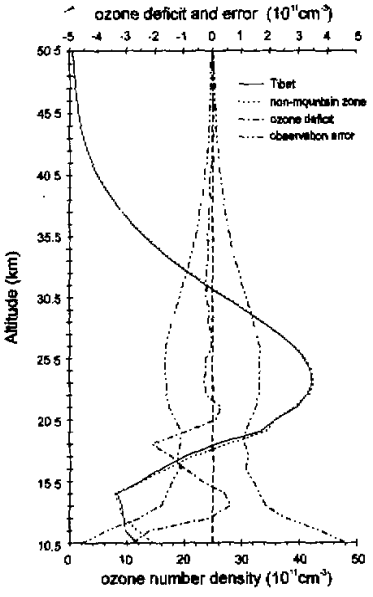

Fig. 1. Annual ozone over Tibet and the non-mountain zone, local ozone deficit and measurement error profiles in number density ($10^{11}cm^{-3}$). Solid line is the ozone over Tibet, dotted line the ozone over non-mountain zone, dash-dotted line the ozone deficit over Tibet, dash-double dotted line the measurement error.

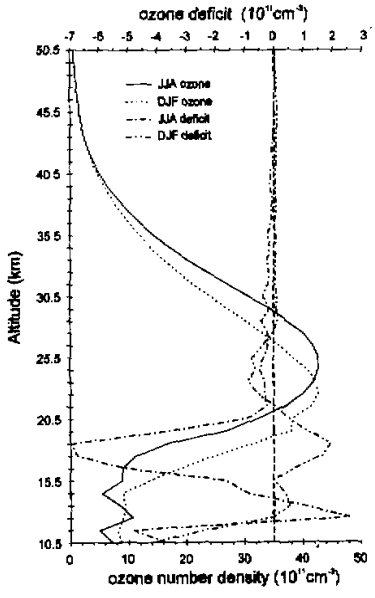

Fig. 2. Seasonal ozone and deficit over Tibet in number density ($10^{11}cm^{-3}$). Solid line is the ozone in summer (JJA), dotted line the ozone in winter (DJF), dash-dotted line the ozone deficit in JJA, dash-double-dotted line the ozone deficit in DJF.

Firstly, looking at the measurement error range in Fig. 1, the observation has higher reliability above 14.5 km a.s.l. with errors in $\pm 1.8 \times 10^{11}$cm^{-3} and the observation is less reliable below this level, with errors up to $\pm 5.0 \times 10^{11}$cm^{-3}. The vertical structure of ozone concentration in Fig. 1 has maximum at about 23.5 km (42.23×10^{11}cm^{-3}) and decreases up- and down-wards. Above 20 km, the ozone concentration over Tibet is quite close to that over the non-mountain zone, and the defference between the ozone number densities over Tibet and the non-mountain zone is less than 0.30×10^{11}cm^{-3} that is within the error range of the observation. The significant feature in Fig. 1 is the Tibet local ozone deficit (negative values) in 15.0–20.0 km. The maximum is at about 18.5 km, -2.12×10^{11}cm^{-3}, and it is out of the error range (1.12×10^{11}cm^{-3}). Below 14.5 km, the ozone concentration and deficit profiles have irregular and discontinuous features with large error range due to the influence of clouds and other low altitude systems. Integrating the ozone profiles in 10.5–50.5 km, the Tibet column total ozone, the non-mountain zone total ozone and the total deficit are obtained as 264.22, 268.86 and −4.62 DU, respectively. Therefore, the column total ozone in 10.5–50.5 km over Tibet is less than the non-mountain zone on annual basis.

A stronger total ozone deficit over Tibet in summer than in winter was revealed by Zou (1996). Therefore, it is important to exam this feature of ozone deficit from the vertical ozone structure over Tibet. Fig. 2 illustrates the vertical ozone and the local deficit profiles over Tibet in winter and summer seasons. The profiles are made from the averaging monthly profiles in June-July-August months (JJA) for summer and in December-January-February months (DJF) for winter. The seasonal deficit profiles are calculated by subtracting the seasonal profiles over the non-mountain zone from those over Tibet. In Figure 2, the maximum of vertical ozone concentration has much higher altitude, 24.5 km, in summer (JJA) than 22.5 km in winter, and the maximum concentrations in summer and winter, 42.57×10^{11}cm^{-3} and 42.59×10^{11}cm^{-3}, are approximately the same. At the level of maximum ozone deficit on

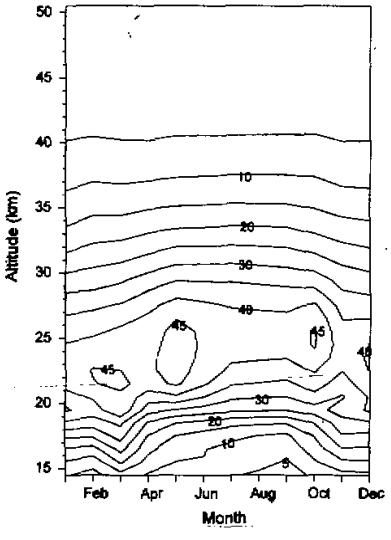

Fig. 3. Monthly variation of ozone concentration over Tibet, in number density (10^{11}cm^{-3}). Contour interval is 5×10^{11}cm^{-3}.

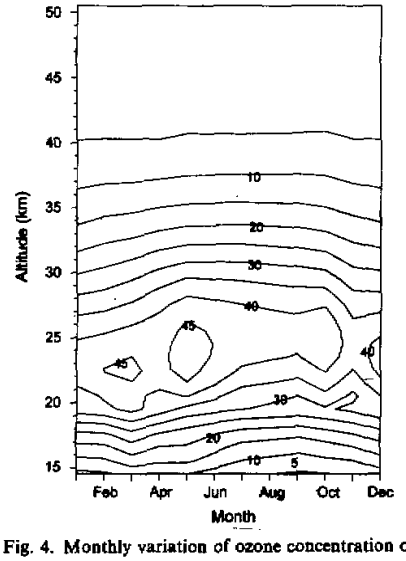

Fig. 4. Monthly variation of ozone concentration over the non-mountain zone, in number density (10^{11}cm^{-3}). Contour interval is 5×10^{11}cm^{-3}.

year-round basis (Fig. 1), 18.5 km, the summer ozone over Tibet is much lower than that over the non-mountain zone, while the winter ozone behaves adversely. The ozone deficit at this altitude, 18.5 km, has negative value, $-6.97 \times 10^{11}cm^{-3}$, in summer and positive value, $1.95 \times 10^{11}cm^{-3}$, in winter. The integration of the seasonal profiles in 10.5–50.5 km over Tibet and the non-mountain zone results in 256.99 DU for the Tibet summer total ozone, 270.30 DU for the non-mountain summer total zone, −13.31 DU for the Tibet summer ozone deficit, 260.27 DU for the Tibet winter total ozone, 260.75 DU for the non-mountain winter total ozone and −0.48 DU for the Tibet winter ozone deficit. From the integrated total column ozone, it is clear that the total ozone in 10.5–50.5 km over Tibet has greater deficit in summer than in winter. This conclusion is identical with Zou's work (1996).

2. *Monthly Variation of Vertical Ozone Profile*

Table 1. The Monthly Maximum Ozone Concentration ($10^{11}cm^{-3}$) and its Altitude (km) over Tibet and the Non-mountain Zone (Non-M)

		Jan	Feb	Mar	Apr	May	Jun	Jul	Aug	Sep	Oct	Nov	Dec
Tibet	Alt.	22.5	22.5	21.5	22.5	23.5	24.5	24.5	25.5	25.5	25.5	24.5	23.5
Ozone	Max.	42.3	45.3	46.0	44.1	47.2	44.4	41.8	41.7	41.7	45.6	37.2	40.7
Non-M	Alt.	22.5	22.5	22.5	23.5	23.5	24.5	24.5	25.5	25.5	24.5	24.5	23.5
Ozone	Max.	42.6	45.1	45.8	43.7	47.6	44.9	42.5	41.9	41.5	44.4	37.4	42.5

The most important feature of the Tibet total ozone is the May maximum of ozone deficit that is not simultaneous with the October minimum of total ozone concentration (Zou, 1996). Averaging the vertical ozone profiles in each month, monthly variations of vertical ozone concentration are plotted in Fig. 3 and 4 for Tibet and the non-mountain zone, respectively. The altitude range is chosen as 14.5–50.5 km for the figures because of the large observation errors in 10.5–14.5 km. Fig. 3 and 4 show great ozone concentrations over $30 \times 10^{11}cm^{-3}$, existing in 18–28 km. The detailed statistics for the monthly variation of maximum ozone concentration is listed in Table 1. In Table 1, the locations of maximum ozone concentration over Tibet and the non-mountain zone stay at the lowest altitude, 21.5–22.5 km, in winter and spring, lift to 23.5 km in later spring (The lifting in Tibet is one month later than in the non-mountain zone.), continue lifting from 24.5 km to 25.5 km in summer, descend to 24.5 km in autumn (The lifting in Tibet is one month later again.), and continue descending continuously to 23.5 km in early winter. The maximum monthly ozone concentration is largest, over $47 \times 10^{11}cm^{-3}$, in May over both the Tibet and the non-mountain zone. This analysis shows that the ozone concentrations over Tibet and the non-mountain zone at and above the maximum concentration altitude, 22–25 km, have small difference. Carefully comparing the two plots (Figs. 3 and 4), the differences can be found below 20 km down to 15 km in spring, summer and autumn, which the Tibet concentration is less than the non-mountain zone. To view clearly the concentration difference between ozone over Tibet and the non-mountain zone, the monthly ozone deficit distribution is made in Fig. 5 by subtracting ozone concentration over the non-mountain zone from that over the Tibet. From Fig. 5, it is clearly showed that there is no significant concentration difference between the ozone over Tibet and the non-mountain zone above 21 km. A large ozone deficit area exists in 15–20 km in spring, summer and autumn and the deficit maximum ($-7.94 \times 10^{11}cm^{-3}$, 16.5 km) is in May. Integration of the monthly ozone deficit profiles shows the monthly Tibet deficit of column ozone in

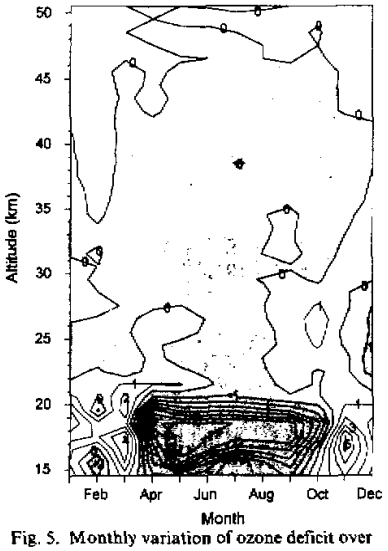

Fig. 5. Monthly variation of ozone deficit over Tibet, in number density ($10^{11}cm^{-3}$). Contour interval is 1(1011cm−3, and the negative area is shaded.

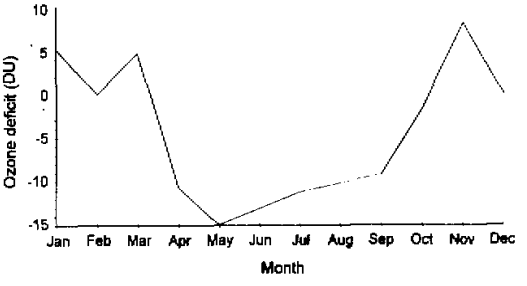

Fig. 6. Monthly variation of column total ozone deficit in 14.5–50.5 km over Tibet, in DU.

14.5–50.5 km (Fig. 6). The column ozone deficits have lower values (larger deficit) in April through September months in 14.5–50.5 km, and the maximum deficit can be found in May as −14.95 DU. However, Fig. 6 gives only the monthly variation of ozone deficit in 15.5–50.5 km over Tibet. This deficit amount is not comparable with the ozone deficit derived from TOMS data (Zou, 1996) because of the differences between the measurement instruments, data periods and thickness of atmospheric column taken in the two studies.

Therefore, the May–month maximum of ozone deficit over Tibet is detected from the SAGE observation in altitude ranges of 14.5–50.5 km, and the deficit occurs in the altitude range of 15–20 km (centered at 16.5 km) where we have reliable measurement.

3. *Temperature and Potential Temperature Profile*

Regarding to the ozone deficit in 15–20 km over Tibet, it is necessary to view the vertical temperature distribution for determining the relationship of the ozone deficit to the atmospheric structure. Fig. 7 gives the monthly vertical distribution of temperature over Tibet by applying the same calculation for ozone distribution. The main feature of the vertical temperature distribution is the temperature inversion (temperature contour 20 K) in 16–21 km that indicates the tropopause. The detailed information of the temperature inversion is given in Table 2. From Fig. 7 and Table 2 it is found that the tropopause temperature inversion shifts a little (17.5–18.5 km) in altitude, but has maximum strength (higher temperatures on both upper and lower sides, lower temperature at the center) in summer and minimum strength in later winter. Therefore, one can conclude that the major ozone deficit over Tibet occurs in the upper troposphere and very close to the tropopause by comparing Fig. 7 with Fig. 5.

Potential temperature is one of the most important atmospheric properties. The isentropic surface (equal potential temperature) can be used as an indicator of equal–mass

surface, so the monthly variation of isentropic surface height can be related to monthly variation of vertical mass transfer. Relatively high isentropic surfaces should have experienced an upward mass transfer and the low ones should have had a downward transfer. Therefore, the monthly potential temperature variation is calculated to study the vertical mass motion over Tibet (Fig. 8). To focus on the maximum ozone deficit, the altitude range is set in 14.5–24.5 km in Fig. 8. Because the vertical ozone distribution has maximum at c.a. 22.5 km (Tab. 1 and Fig. 3), an upward mass transfer should result in ozone decrease in 14.5–20.5 km. This is because the upward mass transfer brings poor-ozone air from low altitude to substitute the rich-ozone air aloft. In Fig. 8, the isentropic surfaces above 14.5 km have the variation characteristics: 1) having minimum altitude in February; 2) lifting 1–2 km upward until July maximum altitude during February to July; and 3) descending back to the minimum altitude in February. The seasonal variation of the isentropic surfaces decreases with altitude. Above 20 km, the variation becomes smooth with amplitude smaller than 0.5 km. In a general view, the upward mass transfer above 14.5 km from February to July can contribute to ozone losing in 15.5–20.5 km in spring and summer, and autumn is the period for recovering the ozone losing (see Fig. 5). The evidence of the upward mass transfer can be also found from the higher altitude of maximum ozone concentration in summer than winter months (Fig. 2). Therefore, the upward mass transfer below the height of maximum ozone concentration in February–July can be the cause of ozone deficit in 15.5–20.5 km in this period.

Table 2. The Monthly Variation of Altitude (km) and Temperature (K) of Inversion

	Jan	Feb	Mar	Apr	May	Jun	Jul	Aug	Sep	Oct	Nov	Dec
Alt.	18.5	18.5	18.5	18.5	18.5	18.5	17.5	17.5	17.5	17.5	18.5	18.5
Temp	208.2	210.5	209.6	207.9	205.7	204.2	202.5	202.9	203.4	205.8	208.5	208.0

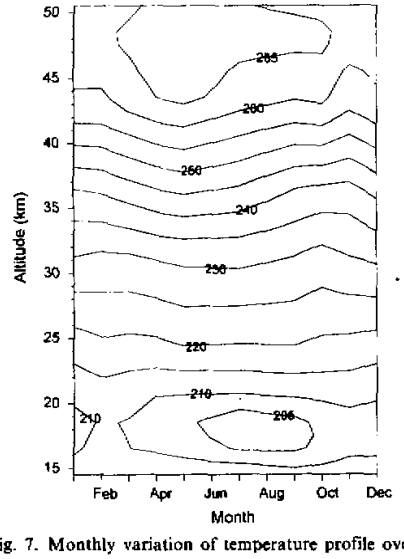

Fig. 7. Monthly variation of temperature profile over Tibet, in K. Contour interval is 5 K.

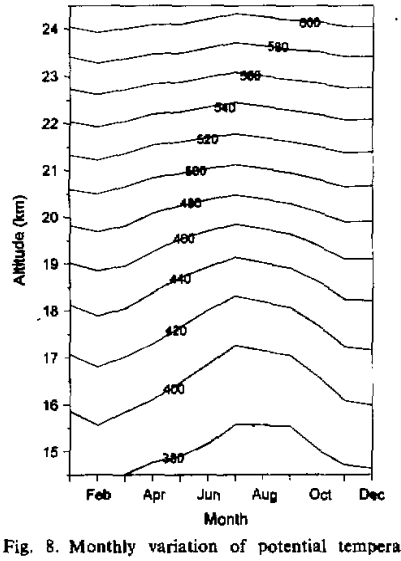

Fig. 8. Monthly variation of potential temperature over Tibet, in K. Contour interval is 20 K.

IV. CONCLUDING REMARKS

After the study described above, conclusions can be made:

1) the characteristics of column total ozone deficit over Tibet is confirmed by SAGE observation in 10.5–50.5 km;

2) the summer ozone deficit over Tibet is stronger than the winter deficit;

3) the altitude of maximum ozone deficit over Tibet is centered at 18.5 km in the upper troposphere and close to the tropopause, in year–round and summer ozone profile;

4) the largest ozone deficit is in May months in column ozone of 14.5–50.5 km and vertical maximum at 16.5 km; and

5) the mass transfer analyzed from potential temperature variation is related to the ozone deficit over Tibet.

The authors have special thanks to Profs. Ye Duzheng, Gao Dengyi, Qu Shaohou and Song Zhengshan, at the Institute of Atmospheric Physics, Chinese Academy of Sciences, for their helpful suggestion and discussion on this work. The authors also wish to thank NASA / NCDS, NCAR / NMC and their staffs for their kind supply and help on SAGE and Meteorological data.

REFERENCES

Attmannspacher, W., J. de la Noe, D. de Muer, J. Lenoble, G. Megie, J. Pelon, P. Pruvost, and R. Reiter (1989), European validation of SAGE II ozone profiles, *J. Geophys. Res.* **94:** D6, 8461–8466.

Bojkov, R. D., L. Bishop, W. J. Hill, G. C. Reinsel, and G. C. Tiao (1990), A statistical trend analysis of revised Dobson total ozone data over the Northern Hemisphere, *J. Geophys. Res.*, **95:** 9785–9807.

Cunnold, D.M., W.P. Chu, R.A. Barnes, M.P. McCormick, and R.E. Veiga (1989), Validation of SAGE II Ozone Measurements, *J. Geophys. Res.*, **94:** D6, 8447–8460.

Farman, J. G. and J. D. Shaklin (1985), Large losses of total ozone in Antarctic reveal seasonal ClO_x / NO_x interaction, *Nature*, **315:** 207–210.

Johnston, H (1971), Reduction of stratospheric ozone by nitrogen oxide catalysts from the supersonic transport exhaust, *Science*, **173:** 517.

Molina, M. J. and F. S. Rowland (1974), Stratospheric sink for chloroflouromethanes: chlorine atomic–catalysed destruction of ozone, *Nature*, **249:** 810.

NASA (1992), Greenhouse effect detection experiment CDROM – A NASA contribution to the international space year (ISY), NASA NCDS, USA, March 1992.

Reinsel, G. C., G. C. Tiao, D. J. Wuebbles, J. B. Kerr, A. J. Miller, R. M. Nagatani, L. Bishop and L. H. Ying (1994), Seasonal trend analysis of published ground–based and TOMS total ozone data through 1991, *J. Geophys. Res.*, **99:** D3, 5449–5464.

Stolarski, R., R. Bojkov, L. Bishop, C. Zerefos, J. Staehelin and J. Zawodny (1992), Measured trends in stratospheric ozone, *Science*, **256:** 342–349.

Wang, Guiqin (1985), Atmospheric ozone research, Science Press, Beijing, 11. (in Chinese)

WMO (1985), Atmospheric ozone 1985, Assessment of our understanding of process controlling its distribution and change, Global ozone research and monitoring project, rept. 16, Geneva, 333.

Zhou, Xiuji and Chao Luo (1994), Ozone valley over Tibetan Plateau, *Acta Meteorologica Sinica*, **8(4):** 505–506.

Zou, Han (1996), Seasonal variation and trends of TOMS ozone over Tibet, *Geophys. Res. Lett.*, **23(9):** 1029–1032.